

# Notch regulates cell fate and dendrite morphology of newborn neurons in the postnatal dentate gyrus

Joshua J. Breunig<sup>\*†</sup>, John Silbereis<sup>‡</sup>, Flora M. Vaccarino<sup>\*‡</sup>, Nenad Šestan<sup>\*†</sup>, and Pasko Rakic<sup>\*†§</sup>

<sup>\*</sup>Department of Neurobiology, <sup>†</sup>Kavli Institute for Neuroscience, and <sup>‡</sup>Child Study Center, Yale University School of Medicine, New Haven, CT 06520

Contributed by Pasko Rakic, October 25, 2007 (sent for review September 15, 2007)

The lifelong addition of neurons to the hippocampus is a remarkable form of structural plasticity, yet the molecular controls over proliferation, neuronal fate determination, survival, and maturation are poorly understood. Expression of Notch1 was found to change dynamically depending on the differentiation state of neural precursor cells. Through the use of inducible gain- and loss-of-function of Notch1 mice we show that this membrane receptor is essential to these distinct processes. We found *in vivo* that activated Notch1 overexpression induces proliferation, whereas  $\gamma$ -secretase inhibition or genetic ablation of Notch1 promotes cell cycle exit, indicating that the level of activated Notch1 regulates the magnitude of neurogenesis from postnatal progenitor cells. Abrogation of Notch signaling *in vivo* or *in vitro* leads to a transition from neural stem or precursor cells to transit-amplifying cells or neurons. Further, genetic Notch1 manipulation modulates survival and dendritic morphology of newborn granule cells. These results provide evidence for the expansive prevalence of Notch signaling in hippocampal morphogenesis and plasticity, suggesting that Notch1 could be a target of diverse traumatic and environmental modulators of adult neurogenesis.

adult neurogenesis | Mash1 | proneural | stem cell

The great majority of neurons in the mammalian brain are generated prenatally (1–3). Despite the existence of neural precursor cells in almost all regions of the adult brain, neurons are actively generated in large numbers only in the dentate gyrus (DG) of the hippocampus and subependymal zone (SEZ) of the lateral ventricles. Although much progress has been made in identifying factors regulating these progenitors (4–6), our knowledge of the molecular mediators that permit neurogenesis in these regions remains limited (3, 7).

Notch is a transmembrane receptor (Notch1–4 in mammals) that upon ligand binding (Jagged1/2 or Delta 1–4 in mammals) is cleaved, releasing the intracellular portion (NICD) that translocates to the nucleus (8, 9). There, it binds Rbbsuh (also known as RBPjk) and the coactivator Mastermind to initiate transcription of target genes (10). The role of Notch in neural progenitors during postnatal hippocampal neurogenesis has not been investigated *in vivo*.

Here, we used an inducible form of Cre recombinase spatially restricted to astroglia. Here, we report that ablation or overexpression of Notch1 in glial fibrillary acidic protein (Gfap)-expressing astroglial cells dramatically affects the proliferation, cell fate, and survival of progenitors as well as the maturation of newly generated neurons, displaying the central role of Notch1 in postnatal hippocampal plasticity.

## Results

**Notch1 and Notch-Signaling Components Are Expressed in the Postnatal Hippocampal Neurogenic Niche.** We first examined the expression pattern of Notch1 in the postnatal murine forebrain by using *in situ* hybridization. Notch1 signal was enriched in the germinal areas, which include the SEZ and the subgranular zone (SGZ) of the DG (Fig. 1A). Multiple components of the Notch pathway, including Hes1, Rbbsuh, Dll-1, and Jag1, were also expressed in this region (supporting information (SI) Fig. 6). An

antibody raised against the intracellular portion of Notch (NICD) was used to precisely examine the cell types expressing Notch and determine the subcellular localization of NICD. This antibody should recognize all forms of Notch1 containing the intracellular aspect of the protein, including full-length Notch1 and NICD. NICD was present in the cytoplasm of many Gfap<sup>+</sup> cells including the radial glia-like neural progenitors that reside in the SGZ of the DG ( $94 \pm 2\%$  of Gfap<sup>+</sup> cells were NICD<sup>+</sup>,  $n = 231$  cells, three animals; Fig. 1B and C). This pattern did not significantly change in all ages examined from P5 to 6 months (data not shown). Among the Doublecortin<sup>+</sup> (Dcx<sup>+</sup>) young neurons, NICD was typically absent from the nucleus of the most immature cells—as evidenced by their lack of a prominent process or dendritic arborization in comparison with neighboring, ramified Dcx<sup>+</sup> cells (Fig. 1C, SI Fig. 7, data not shown). These more immature Dcx<sup>+</sup> cells (also known as Type-3 cells) are thought to be a subpopulation of the transit-amplifying cells (TACs) in the postnatal brain (11, 12). However, mature Dcx<sup>+</sup> cells exhibited higher levels of nuclear NICD, which was positively correlated with the age/maturation state of the cell as determined by dendritic complexity, size, and nuclear localization of the cdk inhibitor p27Kip1, an early indicator of postmitotic status (SI Fig. 7).

Embryonically, as the radial glial cells differentiate, proneural basic helix–loop–helix genes are activated to initiate cell cycle withdrawal and migration in cells with low Notch activity (13, 14). We found a similar pattern as the proneural genes *Ascl1* and *Ngn2* were expressed sporadically in the SGZ but not in the hilus, granule cell layer, or molecular layer (Fig. 1D, SI Figs. 6 and 8). *Ngn2* was also found to frequently colocalize with *Dcx* (SI Fig. 6). *Ascl1*-expressing cells were present in substantially greater numbers compared with *Ngn2* (data not shown), which is consistent with previous reports (15), and they were largely proliferative in nature as determined by colocalization with the cell cycle marker *Ki67* (SI Fig. 8). There was frequently an inverse correlation between the intensity of cytoplasmic NICD and *Ascl1* immunostaining (Fig. 1D). However, clear nuclear localization of NICD in precursors was rare but was found almost exclusively in *Ascl1*<sup>+</sup> radial glia (SI Fig. 9). Taken together, the expression of Notch1 in hippocampal radial glia-like precursors and its down-regulation in TACs suggests that Notch1 is involved in the regulation of SGZ radial glia differentiation into committed neural progenitor cells during postnatal neurogenesis in the DG. Furthermore, the positive correlation between more mature NeuN<sup>+</sup>/Dcx<sup>+</sup> cells and nuclear NICD intensity suggests that Notch signaling may also be important for newborn neuron maturation.

Author contributions: J.J.B., J.S., F.M.V., N.Š., and P.R. designed research; J.J.B., J.S., and N.Š. performed research; J.J.B., J.S., F.M.V., and N.Š. contributed new reagents/analytic tools; J.J.B., F.M.V., N.Š., and P.R. analyzed data; and J.J.B., F.M.V., N.Š., and P.R. wrote the paper.

The authors declare no conflict of interest.

<sup>§</sup>To whom correspondence should be addressed. E-mail: pasko.rakic@yale.edu.

This article contains supporting information online at [www.pnas.org/cgi/content/full/0710156104/DC1](http://www.pnas.org/cgi/content/full/0710156104/DC1).

© 2007 by The National Academy of Sciences of the USA

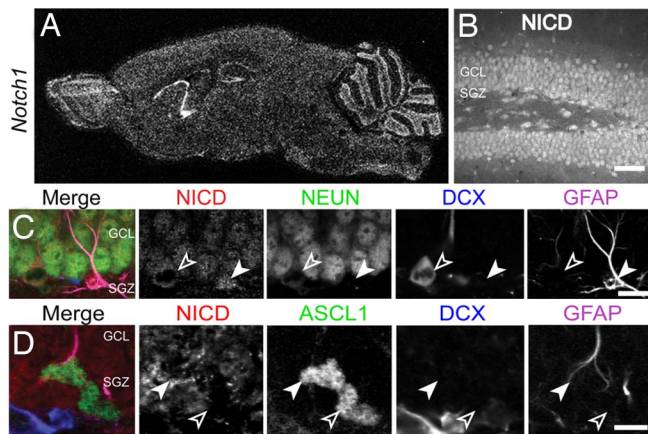


**Fig. 1.** Notch1 and Ascl1 expression in the postnatal hippocampus. (A) *In situ* hybridization for Notch1 mRNA. (B) Low-magnification confocal image of the immunohistochemical localization of Notch1 in P24 hippocampal coronal sections. Immunoreactivity is present in virtually all mature neurons and astrocytes. (C) Confocal image of a section stained for NICD (red), NeuN (green), Dcx (blue), and Gfap (magenta) taken through the dentate gyrus. There is prominent colocalization of NeuN and NICD in mature neurons as well as significant localization of NICD in the cytoplasm of Gfap<sup>+</sup> astrocytes (filled arrowhead) and an absence of NICD in the nearby Dcx<sup>+</sup> cell (empty arrowhead). (D) Immunostaining for NICD (red), Ascl1 (green), Dcx (blue), and Gfap (magenta). Ascl1<sup>+</sup> doublet with one Ascl1<sup>+</sup> nucleus colocalizing with Gfap (filled arrowhead) and the other Gfap<sup>-</sup> (empty arrowhead). NICD did not colocalize with the mostly nuclear Ascl1 protein in either case. GCL, granule cell layer; SGZ, subgranular zone. (Scale bars: B, 100  $\mu$ m; C and D, 10  $\mu$ m.)

**Genetic Manipulation of Notch1 Regulates Proliferation of Gfap<sup>+</sup> Progenitor Cells *in Vivo*.** Because of the high toxicity of Notch-related side effects in the gut following the administration of  $\gamma$ -secretase inhibitors (GSIs) and because GSIs can potentially interfere with a host of signaling pathways, injection of GSIs allows for only an acute observation of the effects of chemical inhibition of Notch signaling (16, 17). Thus, we investigated the Notch signaling pathway further in a more precise, genetic manner. Mice that express a tamoxifen-inducible form of Cre recombinase under the human Gfap promoter (GCE) (18) were crossed with either loxP-flanked Notch1 mice (19) or, conversely, with conditional NICD transgenic mice (20) to conditionally ablate (GCE; Notch1<sup>fl/fl</sup> hereafter referred to as “Notch1 cKO” mice) or overexpress activated Notch1 (GCE; NICD hereafter referred to as “NICD Tg” mice) in Gfap<sup>+</sup> glial cells and all of their progeny on induction of Cre recombination (Fig. 2 A and B). A dose of 1 mg of tamoxifen was given at postnatal day (P) 10, P12, and P14 to induce recombination. This dosing paradigm was chosen because it limited outward signs of toxicity, permitted mice to gain weight normally, and allowed 100% survival of animals while permitting recombination as determined by reporter expression in significant numbers of Gfap<sup>+</sup> cells (Fig. 2C). The control group in all experiments consisted of littermates that were either tamoxifen-treated GCE<sup>+</sup>; Notch1<sup>+/+</sup>, GCE; NICD<sup>-</sup>, GCE<sup>-</sup>; NICD<sup>+/+</sup>, or GCE<sup>-</sup>; Notch1<sup>fl/fl</sup> mice, or vehicle-treated Notch1 cKO or NICD Tg mice (Fig. 2 A and B). No significant differences in proliferation or neuronal differentiation were noted between these groups at the time points examined (data not shown), indicating that Cre toxicity was properly controlled for (21). The efficacy of recombination in Notch1 cKO and NICD Tg mice was assessed by RT-PCR for Hes5. Levels of hippocampal Hes5 mRNA showed equal and opposite changes when compared with control mice (SI Fig. 10). This is consistent with the role of Hes5 as one of the primary effectors of Notch signaling and displays the effectiveness of these inducible mice in recombination of nonreporter,

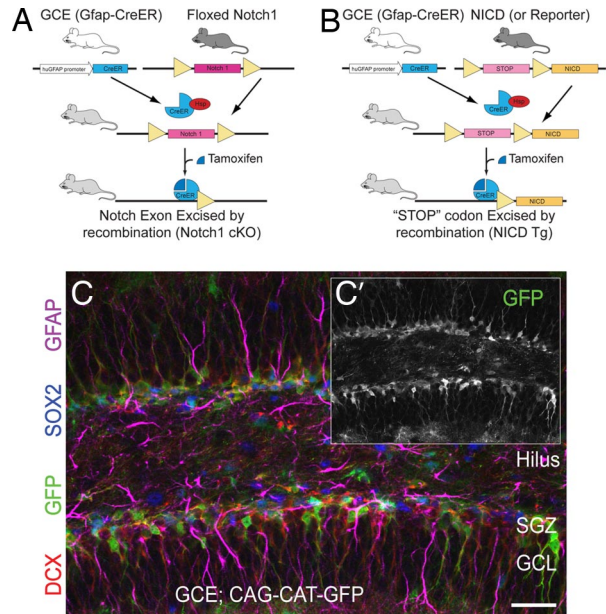


**Fig. 2.** Cre-mediated manipulation of Notch1. (A and B) Schematic of mouse breedings and ligand-induced Cre recombination. (A) GCE mice are crossed with loxP-flanked (“floxed”) Notch1 mice. GCE; Notch1<sup>fl/fl</sup> mice are given tamoxifen, causing the Cre-ERT2 fusion protein—which is otherwise bound to heat shock protein 90 in the cytoplasm and thus is inactive—to translocate to the nucleus where it recombines paired loxP sites, ablating the Notch1 protein. (B) GCE mice are crossed with NICD transgenic mice. GCE; NICD mice are given tamoxifen, causing nuclear translocation of the CreER protein which recombines the loxP sites, excising the “STOP” codon and inducing NICD protein transcription and translation. (C) Three doses of Tamoxifen induce recombination in a significant population of SGZ cells as determined by reporter expression (GFP, green). (Scale bar: C, 50  $\mu$ m.)

floxed alleles. Similarly, immunostaining for NICD generally showed the expected cell autonomous change in Notch protein levels when used in combination with GFP reporter staining in the Notch1 cKO; GFP and NICD Tg; GFP mice (SI Fig. 10).

Compared with controls, Notch1 cKO mice killed 1 week after the final tamoxifen treatment displayed a modest but significant drop in proliferation in the hilus (Fig. 3 B, C, and E). This was similar to *in vivo* results obtained with gamma secretase inhibitors (SI Fig. 11). Rather remarkably, there was a dramatic and widespread 3- to 4-fold increase in Ki67<sup>+</sup> cells in NICD Tg mice, which included an overall change in the pattern of proliferation as marker positive cells were widely present in the hilus and molecular layer, regions not noted for such high levels of proliferation at this age (Fig. 3 D and E). We then performed cell cycle analysis by using a Ki67/iododeoxyuridine (IdU) double-labeling method, which allows for cell cycle exit analysis due to the 24-h survival period after IdU injection, allowing some cells to enter G<sub>0</sub> after incorporating the thymidine analogue into their DNA—while others reenter (22). Cells exiting the cycle should be IdU<sup>+</sup>/Ki67<sup>-</sup>, whereas reentering cells would be IdU<sup>+</sup>/Ki67<sup>+</sup>. The percentage of cells exiting the cell cycle in the SGZ (number of cells IdU<sup>+</sup>/Ki67<sup>-</sup> divided by number of cells IdU<sup>+</sup>) was 42  $\pm$  2% in controls vs. 73  $\pm$  6% in Notch1 cKO or 4  $\pm$  2% in NICD Tg mice (Fig. 3F). Also, compared with controls and NICD Tg mice, fewer Gfap<sup>+</sup> cells proliferated in the IdU was given (9  $\pm$  1% in Notch1 cKO mice vs. 20  $\pm$  1% in controls;  $P < 0.001$ ; Fig. 3G).

Next, double immunolabeling was performed for IdU with chlorodeoxyuridine (CldU), another marker of DNA synthesis, which had been injected at P16, a week before IdU (injected at P23), and two days after the final tamoxifen injection was performed at

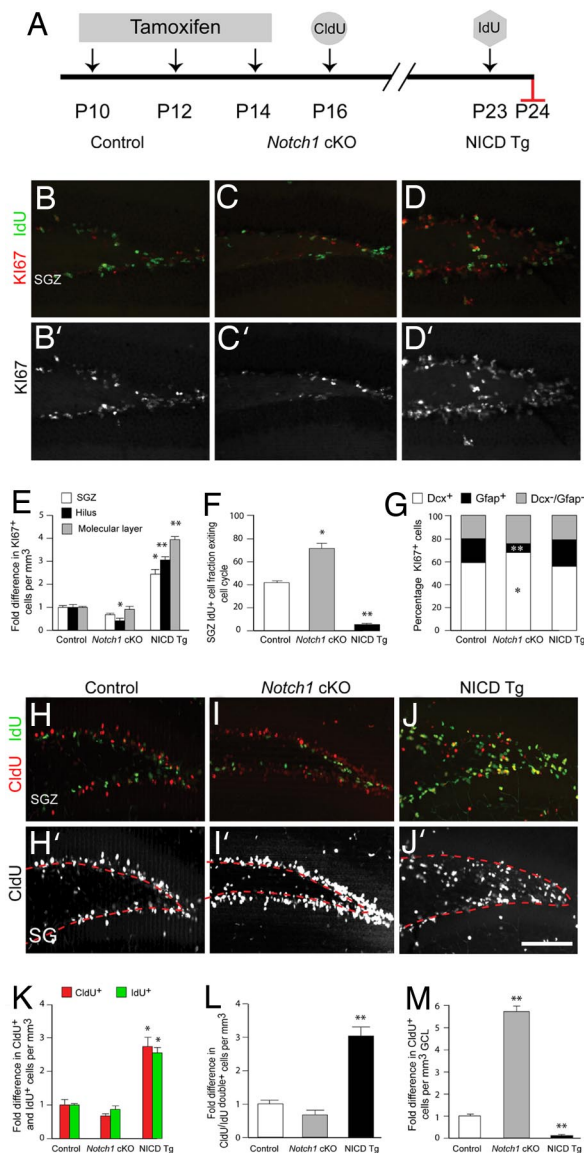


**Fig. 3.** Genetic manipulation of Notch influences cell proliferation, and cell cycle exit. (A) Schematic of the injection paradigm for tamoxifen, CldU, and IdU. (B–D) Ki67 (red)/IdU (green) immunostaining of the dentate gyrus of control (Ctrl), NICD overexpressing (NICD Tg), and Notch1 ablated (*Notch1* cKO) animals. (B'–D') Ki67 signal from B–D shown with enhanced contrast. (E) NICD overexpression drastically increases the number of proliferating cells in the subgranular zone (SGZ), hilus, and molecular layer when compared with controls and *Notch1* cKO groups. The average number of Ki67 positive cells per  $\text{mm}^3$  in control animals was used for normalization. (F) Opposite effects on cell cycle exit are seen when comparing NICD Tg and *Notch1* cKO animals with controls. Significantly more cells leave the cell cycle in *Notch1* cKO animals than in controls or NICD Tg animals where only 7% of cells leave the cell cycle. (G) The phenotype of proliferating cells is skewed in *Notch1* cKO animals where fewer Gfap<sup>+</sup> cells proliferate at a reduced level. (Immunostaining for Dcx/Gfap is not shown for the sake of clarity.) (H–J) CldU (red)/IdU (green) immunohistochemistry on DG tissue sections. (H'–J') CldU signal from H–J is shown with enhanced contrast and the upper limit of the SGZ is labeled with a dotted red line. (K) The number of cells labeled by CldU and IdU increase in the NICD Tg group. The average number of CldU or IdU positive cells per  $\text{mm}^3$  in control animals was used for normalization. (L) CldU/IdU double-positive cell number increases almost threefold in NICD Tg mice over control and *Notch1* cKO animals. The average number of CldU/IdU double-positive cells per  $\text{mm}^3$  in control animals was used for normalization. (M) CldU<sup>+</sup> cells, which synthesized DNA one week before perfusion, remain preferentially in the subgranular zone in NICD Tg animals whereas in *Notch1* cKO animals CldU<sup>+</sup>

P14. Monoclonal antibodies specific for these two thymidine analogues permit specific recognition of either compound in tissue, allowing for the identification of two cohorts of S-phase cells (23). Again, a more than twofold increase in singly labeled CldU<sup>+</sup> or IdU<sup>+</sup> cells was observed in NICD Tg animals compared with controls and *Notch1* cKO mice. When counting CldU and IdU doubly positive cells, which would be indicative of a cell proliferating at both P16 and P23, there was little difference between control animals and *Notch1* cKO mice, but there were 3-fold more CldU<sup>+</sup>/IdU<sup>+</sup> cells in NICD Tg mice compared with both other groups (Fig. 3K). Also, the pattern of labeled cells in *Notch1* cKO mice was altered in that most CldU<sup>+</sup> cells were located in the GCL compared with controls where the proportion of cells in the SGZ vs. GCL was more balanced, indicating increased migration of CldU<sup>+</sup> cells in *Notch1* cKO mice (Fig. 3I and M). Conversely, very few cells appeared to migrate into the GCL in the NICD Tg animals, which would be consistent with the lack of cell cycle exit observed (Fig. 3J and M). These results show that ablating Notch1 in the hippocampus increases the number of progenitors leaving the cell cycle while overexpressing NICD decreases cell cycle exit.

**Alteration of Newborn Neuron Number After Genetic Manipulation of Notch1.** As these groups are genetic mosaics, we bred the Rosa26 (53) and CAG-CAT-GFP (24, 25) reporter strains into each group. By using the same TM delivery protocol and perfusion time as pictured in Fig. 3A, animals in each group were examined for the percentage of SGZ/GCL cells expressing GFP alone (miscellaneous cell types), or in combination with Gfap/Sox2 (astroglia/progenitors), or Dcx (new neurons). In agreement with the cell cycle exit data, Notch1 loss caused a significant increase in new neurons at the expense of progenitors and miscellaneous cell types (Fig. 4B). Conversely, GFP cells in NICD Tg animals overwhelmingly colocalized with Gfap and Sox2, indicating the NICD functions to maintain glial progenitor cells in the SGZ/GCL (Fig. 4B). There was no apparent difference in the average recombination rate or density of recombined cells across the groups or between reporter strains (data not shown). Overall cell death was increased in Cre<sup>+</sup> controls, *Notch1* cKO and NICD Tg animals but examination of the phenotype of dying cells did not yield a pattern indicating that apoptosis was a significant cause of the shift in cell fates (SI Fig. 12). The increase in death seen in Cre<sup>+</sup> controls when compared with Cre<sup>−</sup> animals indicates that Cre toxicity is a significant factor in this assay and thus warrants caution in interpreting survival data from such Cre lines (21). This reciprocal change in cell fate was also seen in comparable young adult mice but the percentages were less than those seen in young animals (Fig. 4C). These results display that cell autonomous manipulation of Notch1 causes a dynamic shift in the ratio of Gfap-positive stem cells versus newborn neurons.

**Notch is a Critical Modulator of Dendritic Arborization in Newly Generated Neurons.** Because of its known effects on neurite outgrowth *in vitro* (26–28), we examined the morphology of newly generated, migrating/differentiating neurons at P37 by using Dcx immunostaining, which labels the maturing dendritic arbor of these young cells. Dcx marks newborn neurons that have been born after tamoxifen treatment at P10, P12, and P14 (11, 18). Despite a lack of significant alteration in the totals number of Dcx<sup>+</sup> cell bodies in NICD Tg and *Notch1* cKO groups (Fig. 5G), there was a remarkable and disproportionate

cells are preferentially found in the granule cell layer. The average number of CldU-positive cells per  $\text{mm}^3$  in control animals was used for normalization. Note  $n = 6$  for each experimental group. Asterisks indicate a statistical difference between experimental groups (\*,  $P < 0.05$ ; \*\*,  $P < 0.001$ ; Student's *t* test: E–G, K–M). Error bars represent SEM. (Scale bars: B–D' and H–J', 100  $\mu\text{m}$ .)



tions to maintain neural stem cells whereas transit-amplifying cells use other signaling pathways or noncanonical Notch signaling (SI Fig. 13). The inability of DN-MAML expression to promote neurogenesis—as is seen after Notch1 ablation in the dentate gyrus—indicates that active neurogenic signals from the microenvironment are needed to promote neurogenesis even in the absence of antineuronal Notch signaling.

**Reactive Neurogenesis in the Postnatal Brain.** It is noteworthy that the pattern of hyperproliferation and morphological plasticity shares similarities with the alterations in neurogenesis seen after trauma, indicating that Notch1 could be an *in vivo* modulator of posttrauma neurogenic responses (37–40). Consistent with this idea, Hes5 and Ascl1 mRNA levels are significantly altered in the SGZ after status epilepticus (41) and ischemia (42). Seizures are known to be one of the most profound stimulators of dentate gyrus neurogenesis. Different experimental models show varying degrees of neurogenesis. Strikingly, increased neurogenesis has been seen concurrently with dramatic dendritic changes in the newborn population (40). Furthermore, because of the transient increase in neurogenesis we observed, it is conceivable that Notch signaling is activated in a graded manner by other potent stimulators of adult neurogenesis such as running (43), ischemia (44), and focal lesion (45). In particular, it has recently been observed that Notch signaling mediates profound postischemia responses (46), and dynamic changes in the expression pattern of Notch-related molecules suggests the involvement of Notch in the postlesion (47) and postischemia neurogenic response (42, 44).

**Dendritic Alterations in Newborn Neurons.** We also show that genetic manipulation of Notch in newborn neurons in the hippocampus alters the dendritic morphology. *In vitro*, Notch was found to have profound effects on the arborization of cortical neurons (26–28). Our results are consistent with this, showing that the dendritic arborization of newly generated neurons is modulated *in vivo* in a dosage-dependent manner based on the cleavage of the Notch receptor. Nevertheless, as Notch signaling levels vary with seizure (41), ischemia (46), and potentially many other stimuli, such changes in dendrite arborization may not be entirely artificial and can reflect physiological challenges. For example, it has recently been shown that voluntary exercise can significantly alter dendritic morphology

and complexity in the dentate gyrus (48, 49), in addition to its known function in neurogenesis (43).

Our data illuminate the complexity of Notch signaling as a whole in the transition from progenitor to mature neuron, displaying its central role during postnatal neurogenesis and raising the possibility that it plays a part in the plasticity resulting from trauma or environmental stimulus. Notch acts in one context to stimulate proliferation of endogenous progenitors, yet in maturing neurons modulates structural plasticity and survival pathways, suggesting that differential clinical manipulation of Notch could aid in multiple aspects of functional recovery after disease, trauma, or pathological aging.

**Note.** After the completion of these experiments, Mizutani *et al.* (50) reported that neural stem cells and committed progenitors display differential levels of Notch signaling in the embryonic brain, consistent with our findings in the postnatal and adult brain.

## Materials and Methods

**Mice.** GCE; R26R/R26R, GCE; Z/EG<sup>+/+</sup>, GCE;<sup>+/+</sup>, <sup>+</sup>/Notch1<sup>fl/fl</sup>, <sup>+</sup>/NICD, GCE;Notch1<sup>fl/fl</sup> (Notch1 cKO), or GCE;NICD (NICD Tg) at the ages noted were administered 75 mg/kg of tamoxifen (Sigma) in corn oil by i.p. injection or oral gavage at the times noted. [No differences were noted between delivery methods, as has been described (51).] Littermates were used as controls. CldU or IdU (Sigma) were given at the times noted as a single i.p. injection equimolar to 100 mg/kg of bromodeoxyuridine. (Most experiments were performed on a C57/BL6 background.) Two-month-old CD1 mice were given i.p. injections of DAPT (Sigma) 200 mg/kg, DBZ (Calbiochem) 4 mg/kg, or DMSO (Sigma) every 12 h for 3 days based on studies characterizing *in vivo* activity (16, 52).

**Statistical Analysis.** A two-tailed unpaired Student's *t* test was used for analyses of all experiments presented in Figs. 3–5. A *P* value < 0.05 was considered significant.

Details on other methods are available in *SI Materials and Methods*.

**ACKNOWLEDGMENTS.** We thank C. Anderson, J. Bao, and M. Pappy for excellent experimental assistance; D. Anderson, J. Aster, M. Colbert, A. Israel, J. Johnson, W. Pear, F. Radtke, and J. Shen for mice and reagents; and J. Arellano, K. Burns, R. Duman, M. Givogri, K. Hashimoto-torii, K. Herrup, C. Y. Kuan, J. Loturco, R. Rasin, M. Sarkisian, T. Town, and members of the P.R. and N.S. laboratories for helpful discussions, technical support, and comments. This work was supported by National Institutes of Health Grants R01 MH067715, HD045481, AG019394, and NS047200; the March of Dimes Birth Defects Foundation Grant FY05-73; and the Kavli Institute.

- Rakic P (1985) Limits of neurogenesis in primates. *Science* 227(4690):1054–1056.
- Bhardwaj RD, *et al.* (2006) From the cover: Neocortical neurogenesis in humans is restricted to development. *Proc Natl Acad Sci USA* 103(33):12564–12568.
- Gage, FH (2000) Mammalian neural stem cells. *Science* 287(5457):1433–1438.
- Lie DC, *et al.* (2005) Wnt signalling regulates adult hippocampal neurogenesis. *Nature* 437(7063):1370–1375.
- Lai K, *et al.* (2003) Sonic hedgehog regulates adult neural progenitor proliferation *in vitro* and *in vivo*. *Nat Neurosci* 6(1):21–27.
- Machold R, *et al.* (2003) Sonic hedgehog is required for progenitor cell maintenance in telencephalic stem cell niches. *Neuron* 39(6):937–950.
- Lledo PM, Alonso M, Grubb MS (2006) Adult neurogenesis and functional plasticity in neuronal circuits. *Nat Rev Neurosci* 7(3):179–193.
- Artavanis-Tsakonas S, Rand MD, Lake RJ (1999) Notch signaling: Cell fate control and signal integration in development. *Science* 284(5415):770–776.
- Schroeter EH, Kisslinger JA, Kopan R (1998) Notch-1 signalling requires ligand-induced proteolytic release of intracellular domain. *Nature* 393(6683):382–386.
- Bray SJ (2006) Notch signalling: A simple pathway becomes complex. *Nat Rev Mol Cell Biol* 7(9):678–689.
- Brown JP, *et al.* (2003) Transient expression of doublecortin during adult neurogenesis. *J Comp Neurol* 467(1):1–10.
- Plumpe T, *et al.* (2006) Variability of doublecortin-associated dendrite maturation in adult hippocampal neurogenesis is independent of the regulation of precursor cell proliferation. *BMC Neurosci* 7:77.
- Britz O, *et al.* (2006) A role for proneural genes in the maturation of cortical progenitor cells. *Cereb Cortex* 16(Suppl 1):i138–i151.
- Castro DS, *et al.* (2006) Proneural bHLH and Brn proteins coregulate a neurogenic program through cooperative binding to a conserved DNA motif. *Dev Cell* 11(6):831–844.
- Pleasure SJ, Collins AE, Lowenstein DH (2000) Unique expression patterns of cell fate molecules delineate sequential stages of dentate gyrus development. *J Neurosci* 20(16):6095–6105.
- van Es JH, *et al.* (2005) Notch/gamma-secretase inhibition turns proliferative cells in intestinal crypts and adenomas into goblet cells. *Nature* 435(7044):959–963.
- Barten DM, *et al.* (2006) Gamma-secretase inhibitors for Alzheimer's disease: Balancing efficacy and toxicity. *Drugs R D* 7(2):87–97.
- Ganat YM, *et al.* (2006) Early postnatal astroglial cells produce multilineage precursors and neural stem cells *in vivo*. *J Neurosci* 26(33):8609–8621.
- Lutolf S, *et al.* (2002) Notch1 is required for neuronal and glial differentiation in the cerebellum. *Development (Cambridge, UK)* 129(2):373–385.
- Yang X, *et al.* (2004) Notch activation induces apoptosis in neural progenitor cells through a p53-dependent pathway. *Dev Biol* 269(1):81–94.
- Breunig JJ, *et al.*, Everything that glitters is not gold: A critical review of analysis of neural precursor / stem cells. *Cell Stem Cell*, in press.
- Chenn A, Walsh CA (2002) Regulation of cerebral cortical size by control of cell cycle exit in neural precursors. *Science* 297(5580):365–369.
- Vega CJ, Peterson DA (2005) Stem cell proliferative history in tissue revealed by temporal halogenated thymidine analog discrimination. *Nat Methods* 2(3):167–169.
- Nakamura T, Colbert MC, Robbins J (2006) Neural crest cells retain multipotential characteristics in the developing valves and label the cardiac conduction system. *Circ Res* 98(12):1547–1554.
- Burns KA, *et al.* (2007) Nestin-CreER mice reveal DNA synthesis by nonapoptotic neurons following cerebral ischemia-hypoxia. *Cereb Cortex* 17(11):2585–2592.
- Sestan N, Artavanis-Tsakonas S, Rakic P (1999) Contact-dependent inhibition of cortical neurite growth mediated by notch signaling. *Science* 286(5440):741–746.
- Berezovska O, *et al.* (1999) Notch1 inhibits neurite outgrowth in postmitotic primary neurons. *Neuroscience* 93(2):433–439.

28. Redmond L, et al. (2000) Nuclear Notch1 signaling and the regulation of dendritic development. *Nat Neurosci* 3(1):30–40.
29. Jones SP, et al. (2003) Maturation of granule cell dendrites after mossy fiber arrival in hippocampal field CA3. *Hippocampus* 13(3):413–427.
30. Gaiano N, Nye JS, Fishell G (2000) Radial glial identity is promoted by Notch1 signaling in the murine forebrain. *Neuron* 26(2):395–404.
31. Tanigaki K, et al. (2001) Notch1 and Notch3 instructively restrict bFGF-responsive multipotent neural progenitor cells to an astroglial fate. *Neuron* 29(1):45–55.
32. Jadhav AP, Mason HA, Cepko CL (2006) Notch 1 inhibits photoreceptor production in the developing mammalian retina. *Development (Cambridge, UK)* 133(5):913–923.
33. Chambers CB, et al. (2001) Spatiotemporal selectivity of response to Notch1 signals in mammalian forebrain precursors. *Development (Cambridge, UK)* 128(5):689–702.
34. Mizutani K, Saito T (2005) Progenitors resume generating neurons after temporary inhibition of neurogenesis by Notch activation in the mammalian cerebral cortex. *Development (Cambridge, UK)* 132(6):1295–1304.
35. Maillard I, et al. (2004) Mastermind critically regulates Notch-mediated lymphoid cell fate decisions. *Blood* 104(6):1696–1702.
36. Weng AP, et al. (2003) Growth suppression of pre-T acute lymphoblastic leukemia cells by inhibition of notch signaling. *Mol Cell Biol* 23(2):655–664.
37. Pierce JP, et al. (2005) Mossy fibers are the primary source of afferent input to ectopic granule cells that are born after pilocarpine-induced seizures. *Exp Neurol* 196(2):316–331.
38. Scharfman HE, Goodman JH, Sollas AL (2000) Granule-like neurons at the hilar/CA3 border after status epilepticus and their synchrony with area CA3 pyramidal cells: Functional implications of seizure-induced neurogenesis. *J Neurosci* 20(16):6144–6158.
39. Parent JM, et al. (2006) Aberrant seizure-induced neurogenesis in experimental temporal lobe epilepsy. *Ann Neurol* 59(1):81–91.
40. Overstreet-Wadiche LS, et al. (2006) Seizures accelerate functional integration of adult-generated granule cells. *J Neurosci* 26(15):4095–4103.
41. Elliott RC, et al. (2001) Differential regulation of basic helix-loop-helix mRNAs in the dentate gyrus following status epilepticus. *Neuroscience* 106(1):79–88.
42. Kawai T, et al. (2005) Changes in the expression of Hes5 and Mash1 mRNA in the adult rat dentate gyrus after transient forebrain ischemia. *Neurosci Lett* 380(1–2):17–20.
43. Zhao C, et al. (2006) Distinct morphological stages of dentate granule neuron maturation in the adult mouse hippocampus. *J Neurosci* 26(1):3–11.
44. Felling RJ, et al. (2006) Neural stem/progenitor cells participate in the regenerative response to perinatal hypoxia/ischemia. *J Neurosci* 26(16):4359–4369.
45. Emery DL, et al. (2005) Newly born granule cells in the dentate gyrus rapidly extend axons into the hippocampal CA3 region following experimental brain injury. *J Neurotrauma* 22(9):978–988.
46. Arumugam TV, et al. (2006) Gamma secretase-mediated Notch signaling worsens brain damage and functional outcome in ischemic stroke. *Nat Med* 12(6):621–623.
47. Givogri MI, et al. (2006) Notch signaling in astrocytes and neuroblasts of the adult subventricular zone in health and after cortical injury. *Dev Neurosci* 28(1–2):81–91.
48. Eadie BD, Redila VA, Christie BR (2005) Voluntary exercise alters the cytoarchitecture of the adult dentate gyrus by increasing cellular proliferation, dendritic complexity, and spine density. *J Comp Neurol* 486(1):39–47.
49. Redila VA, Christie BR (2006) Exercise-induced changes in dendritic structure and complexity in the adult hippocampal dentate gyrus. *Neuroscience* 137(4):1299–1307.
50. Mizutani K, et al. (2007) Differential Notch signalling distinguishes neural stem cells from intermediate progenitors. *Nature* 449(7160):351–355.
51. Joyner AL, Zervas M (2006) Genetic inducible fate mapping in mouse: Establishing genetic lineages and defining genetic neuroanatomy in the nervous system. *Dev Dyn* 235(9):2376–2385.
52. El Mouedden M, et al. (2006) Reduction of Abeta levels in the Sprague Dawley rat after oral administration of the functional gamma-secretase inhibitor, DAPT: A novel non-transgenic model for Abeta production inhibitors. *Curr Pharm Des* 12(6):671–676.
53. Mao X, Fujiwara Y, Orkin SH (1999) Improved reporter strain for monitoring Cre recombinase-mediated DNA excisions in mice. *Proc Natl Acad Sci USA* 96(9):5037–5042.

## Supporting Information Text

**Immunohistochemistry of Sections and TUNEL.** Sixty-micrometer vibratome sections were prepared from 4% paraformaldehyde-fixed brains that were subsequently fixed overnight at 4°C in the same fixative. Free-floating sections were blocked and incubated overnight in blocking solution at 4°C with appropriate primary antibodies (specifics detailed in SI Table 1). Secondary antibodies for quadruple labeling were donkey antispecies conjugated with FITC, Cy3, Cy5, and AMCA. Sections stained for CldU or IdU were pretreated with 2 M HCl for 20 min and neutralized with borate buffer before incubation with primary antibody. Tissue for Ki67 immunostaining was mounted and incubated in Target Retrieval Solution (Dako) for 45 min at 95°C. Bright-field immunohistochemistry was performed by using biotinylated secondary antibodies (Jackson), biotin-avidin peroxidase complex (Vector), and diaminobenzidine (Vector) as the developing agent. TUNEL was performed on mounted sections according to the manufacturer's instructions (Chemicon, Apoptag Kit). Fluorescent images were captured in 1- $\mu$ m optical sections by using a confocal laser-scanning microscope (Zeiss LSM 510 META) direct-coupled to a Chameleon Ultra laser pumped by an 10W Verdi laser (Coherent Laser Group) or an Apotome-equipped Zeiss Axioplan2. Consecutive Z-stacks were taken in most cases to confirm colocalization of markers.

***In Situ* Hybridization.** *In situ* hybridizations were performed on cryosections of 3-month-old postnatal mouse brains. Hybridization solution containing P33-labeled probe was then spread over each section, and a coverslip was placed over this solution and sealed. Slides were then incubated in a humidified chamber at 60°C for at least 16 h. After exposure to film, slides were dipped in NTB2 nuclear track emulsion (Kodak), exposed for ~1 month at 4°C, developed, lightly counterstained with hematoxylin and bis-benzamide, coverslipped in glycerol, and photographed with either dark-field, or bright-field optics.

**Morphometric Evaluation.** Cells were counted by using a modified optical fractionator and stereological image analysis software (Stereo Investigator, MicroBrightField) operating a computer-driven microscope. Areas to be counted were traced at low power and counting frames were selected at random by the image analysis software. To trace the dendritic arbors, 3D reconstruction and analysis software (NeuroLucida, MicroBrightField) was used. Two strategies were used. First, for quantification Dcx+ cell bodies in the SGZ/GCL were counted and then dendrites in the ML were independently reconstructed to avoid sampling biases. Second, individual Dcx+/EGFP+ cells were entirely reconstructed from confocal z stacks. The most ramified examples were chosen for reconstruction as EGFP act to delineate recombined cell populations. For the DG, every twelfth section through the entire extent of the hippocampus was examined and cells counts were expressed as cells per mm<sup>3</sup>.

1. Nguyen L, *et al.* (2006) P27<sup>kip1</sup> independently promotes neuronal differentiation and migration in the cerebral cortex. *Genes Dev* 20:1511-1524.
2. Fishell G. (2006) Loss of a notch activity in the developing central nervous system leads to increased cell death. *Dev Neurosci* . 28(6):517.
3. Breunig JJ, *et al.* (2007) Everything that glitters is not gold: a critical review of analysis of neural precursor / stem cells. *Cell Stem Cell*, in press.
4. Oishi K, *et al.* (2004) Notch promotes survival of neural precursor cells via mechanisms distinct from those regulating neurogenesis. *Dev Biol* 276(1):172-184.
5. Kuo CT, *et al.* (2006) Postnatal deletion of Numb/Numbl like reveals repair and remodeling capacity in the subventricular neurogenic niche. *Cell* 127(6):1253-1264.
6. Androutsellis-Theotokis A, *et al.* (2006) Notch signalling regulates stem cell numbers in vitro and in vivo. *Nature* 442(7104):823-826.
7. Mason HA, *et al.* (2006) Loss of notch activity in the developing central nervous system leads to increased cell death. *Dev Neurosci* 28(1-2):49-57.

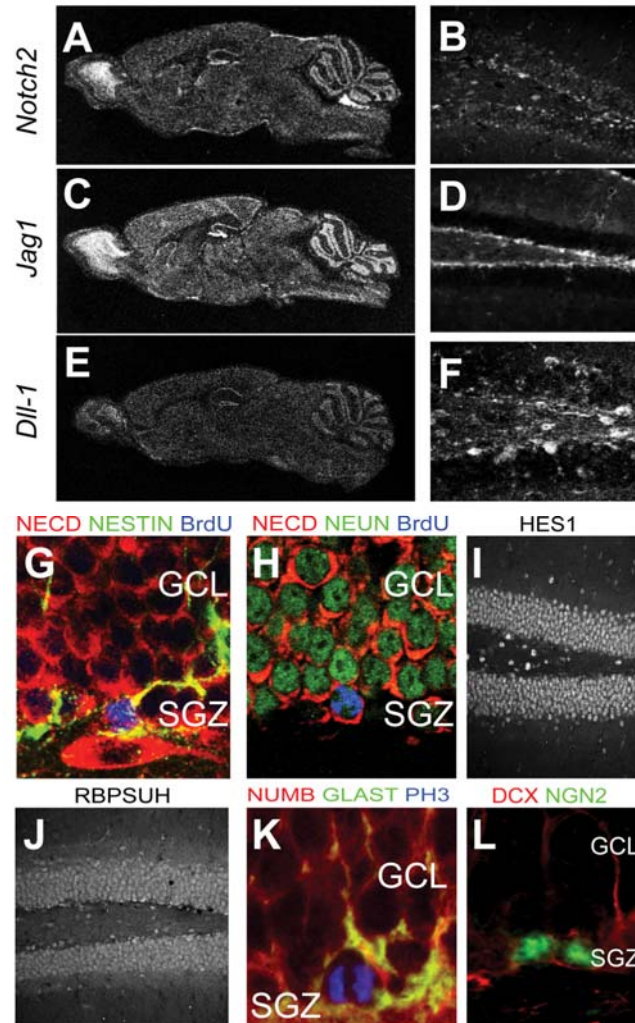


**Fig. 6.** Expression of Notch pathway molecules. (A) *In situ* hybridization for Notch2 mRNA. (B) Low-magnification confocal image of the immunohistochemical localization of Notch2 in hippocampal coronal sections. Notch2 expression was found to be similar to Notch1 pattern. (C) *In situ* hybridization for Jagged1 mRNA. (D) Low-magnification confocal image of the immunohistochemical localization of Jagged1 in hippocampal coronal sections. Jagged1 was enriched in the SGZ in *Dcx*<sup>+</sup> and *Gfap*<sup>+</sup> cells (data not shown). (E) *In situ* hybridization for *Dll-1* mRNA. (F) Low-magnification confocal image of the immunohistochemical localization of *Dll-1* in hippocampal coronal sections. Only scattered cells expressed this ligand—most appearing to be mature neurons based on size and shape. (G) Confocal image of Notch Extracellular Domain (NECD) (red) colocalizing with Nestin (green) and BrdU (blue) 2 hours postinjection. (H) Expression of NECD (red) 3 weeks after injection of BrdU (blue) in a mature NeuN<sup>+</sup> (green) neuron. (I) *Hes1* protein expression mimicks Notch1 protein expression but is localized predominantly to the nucleus as does *Rbpsuh* (J). (K) The Notch-inhibitor *Numb* (red) localizes basolaterally in dividing SGZ radial glia as determined by expression of phosphorylated Histone 3 (Ph-H3, blue) and astrocyte-specific glutamate transporter (GLAST, green). (L) Two Neurogenin-2<sup>+</sup> (*Ngn2*) cells (green) colocalize with *Dcx* (red) in the SGZ.

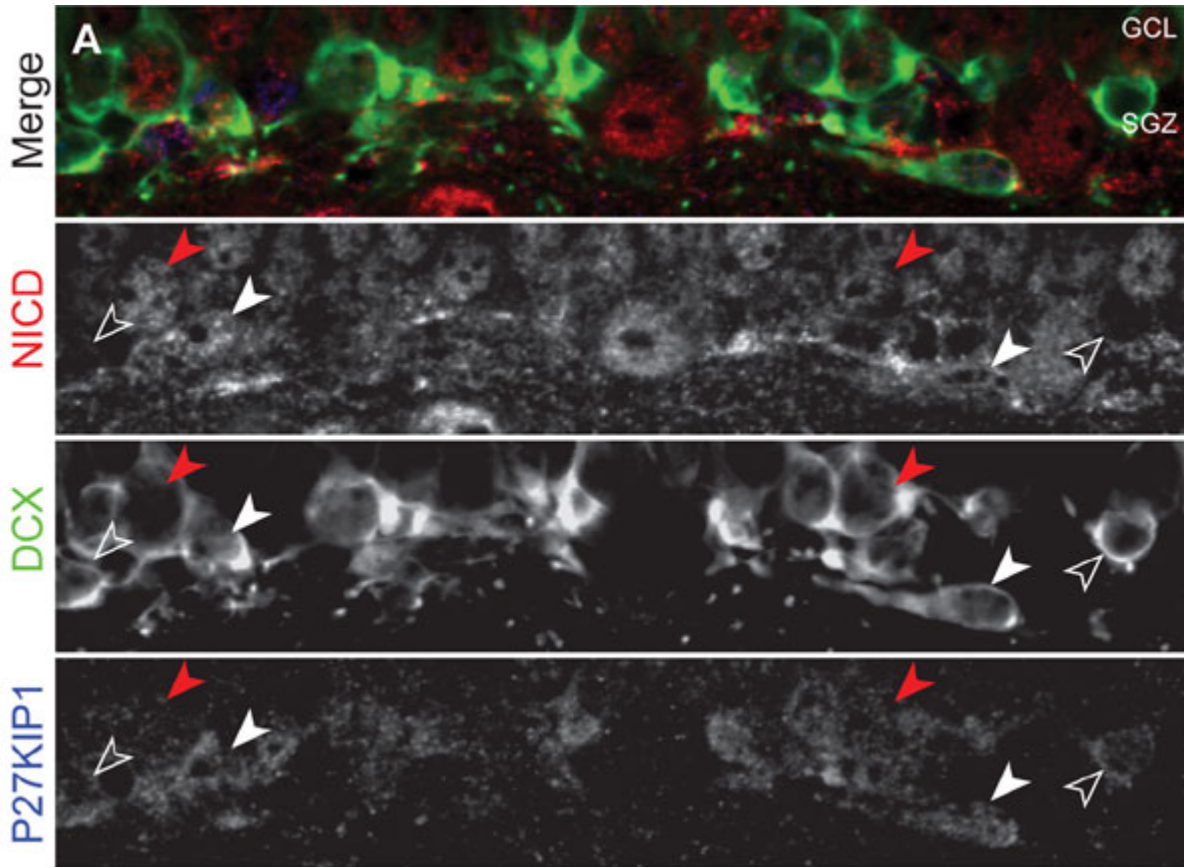


**Fig. 7.** Subcellular distribution of Notch1 is altered as  $Dcx^+$  newborn neurons mature. (A) NICD antibody (red) is absent from the nucleus of the most immature  $Dcx^+$  cells (open arrowheads) in the SGZ. These cells also display weak nuclear localization of the cell cycle inhibitor p27Kip1 (blue). More mature cells begin to accumulate nuclear NICD (white arrowheads) and p27Kip1, indicating cell cycle exit (1). The most mature  $Dcx^+$  cells (red arrowheads) as determined by size and dendrite morphology (not shown) display robust nuclear NICD immunostaining and weaker levels of nuclear p27Kip1-characteristic of maturing, postmigratory neurons.

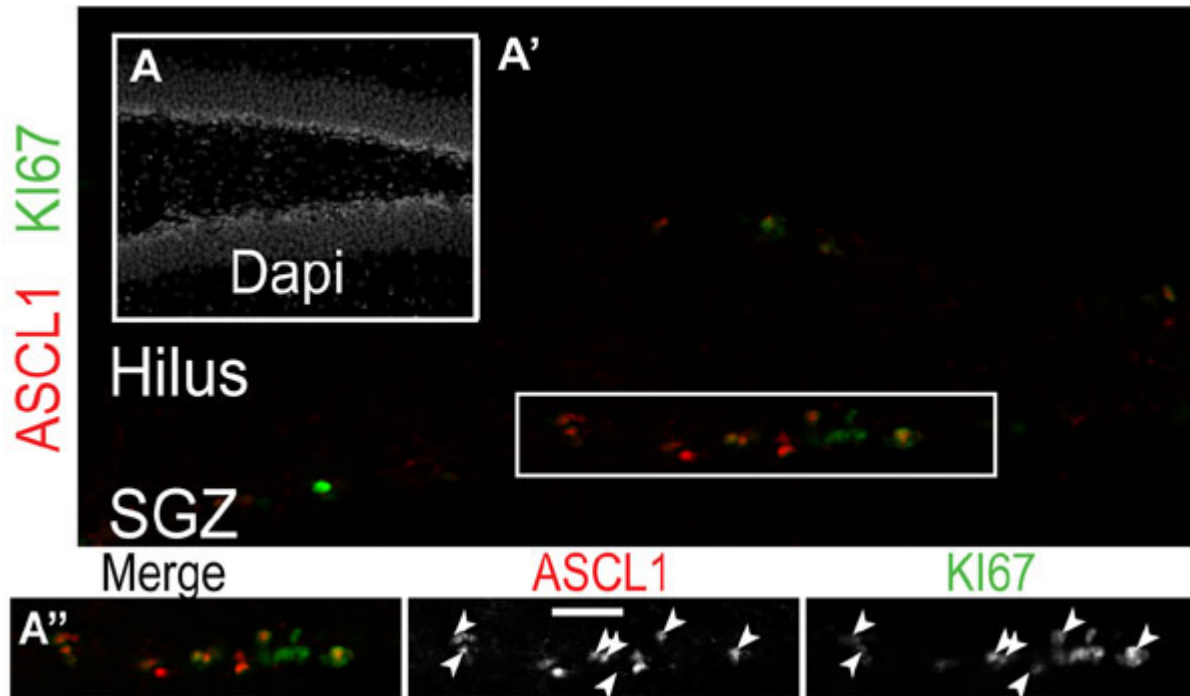


**Fig. 8.** Mash1 is specifically expressed in proliferating SGZ cells. (A-A'') Confocal images of Ascl1 (red), Ki67 (green), and Dapi (blue) staining. (A) Dapi staining of the tissue section under examination. (A') Ki67 and Ascl1 are primarily limited to the SGZ in controls. Boxed region in A' magnified in A''. (A'') Ascl1 and Ki67 largely colocalize in the SGZ (white arrowheads) but several cells remain singly positive for either marker.

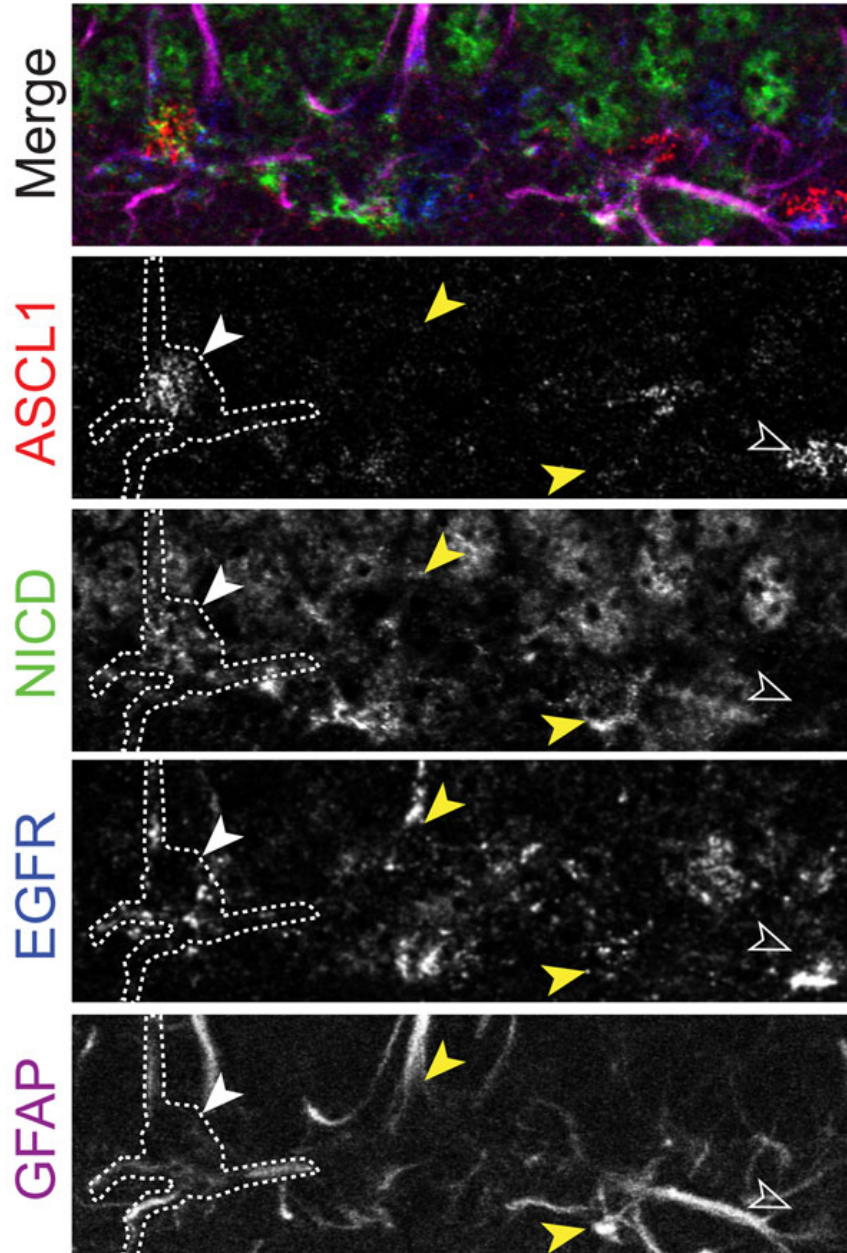


**Fig. 9.** Nuclear NICD is found in a small subset of *Ascl1*-positive SGZ radial glia. A *Gfap*<sup>+</sup> (magenta), *Ascl1*<sup>+</sup> (red) radial glial cell (white arrowhead) with cytoplasmic *Egfr* expression (blue) shows nuclear NICD staining (green) as evidenced by the clear Cajal bodies. Notice the colocalization of *Ascl1* and NICD, identifying the nucleus. This colocalization was very rare, perhaps indicating that nuclear NICD is observable only in a small part of the cell cycle and under tight temporal control. Contrast this with the *Ascl1*<sup>+</sup>/*Egfr*<sup>+</sup> cell that lacks any detectable NICD (open arrowhead). Also visible are two examples of *Ascl1*<sup>-</sup>, *Gfap*<sup>+</sup> astrocytes, which have only minor nuclear staining for NICD but show enrichment of NICD protein in the processes and membrane (yellow arrowheads).

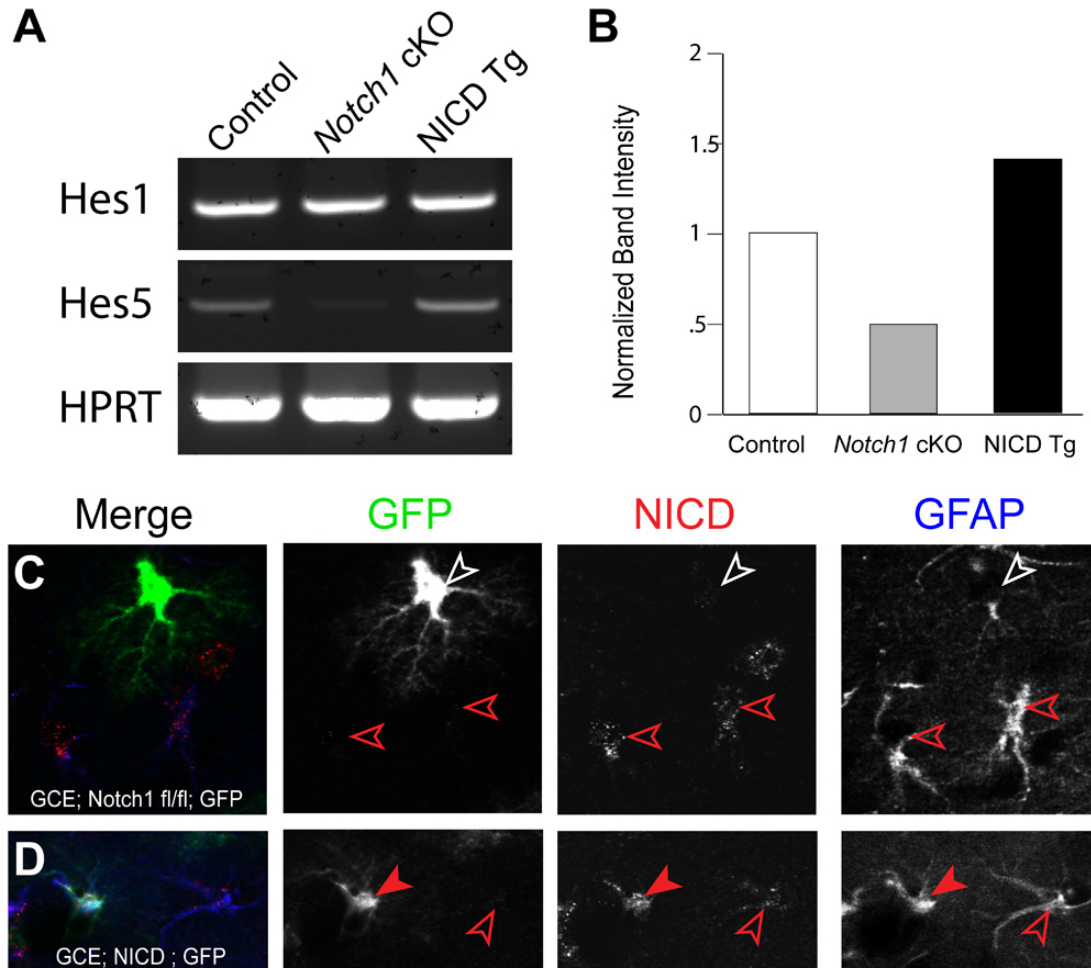


**Fig. 10.** Verification of GCE-inducible mice in recombining nonreporter floxed alleles. (A) RT-PCR for Hes1, Hes5, and HPRT, derived from hippocampal RNA. (B) Normalized expression levels of Hes5 based on bands pictured in A. (C) Immunostaining for NICD shows a lack of detectable Notch1 protein in a GFP+, recombined astrocyte (white-outlined arrowhead) from a GCE; Notch1fl/fl; GFP animal. Reporter-negative astrocytes remain NICD+ (red-outlined arrowheads). (D) GFP+ astrocyte (red arrowhead) in a GCE; NICD; GFP animal shows a notable enrichment of cytoplasmic NICD protein when compared with a GFP- astrocyte (red-outlined arrowhead). The correlation between reporter expression and protein changes as well as reciprocal changes in Hes5 RNA appeared to decrease with age and huGfap-promoter activity (data not shown), perhaps explaining the decrease in significance seen in cell fate alterations seen between P24 animals and 4- to 6-month-old animals in Fig. 4.

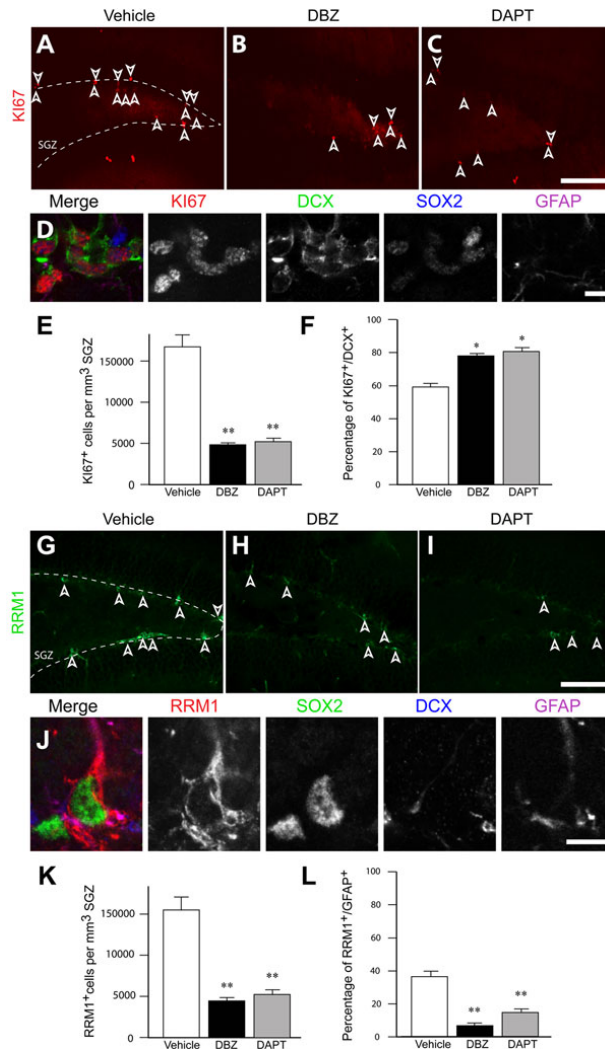


**Fig. 11.**  $\gamma$ -Secretase inhibitors reduce glial proliferation in the subgranular zone. (A-C) Ki67 (red) staining of the subgranular zone (SGZ) in vehicle (A), DBZ (B), and DAPT (C) treated animals. (D) Confocal image of Ki67+(red)/Dcx+(green) cells in the SGZ. (E) The number of Ki67<sup>+</sup> proliferating cells (arrowheads, A-C) is roughly threefold higher in vehicle-treated animals when compared with controls. The average number of Ki67-positive cells per mm<sup>3</sup> in DAPT-injected animals was used for normalization. (F) The relative proportion of proliferating Dcx<sup>+</sup> cells as determined by colocalization with Ki67<sup>+</sup> is increased in DBZ- and DAPT-treated groups. (G-I) Ribonucleotide Reductase M1 (Rrm1, green) subunit staining of the dentate gyrus. (J) Representative image of a Rrm1(red)/Sox2(green)/Gfap(magenta) triple-positive radial glial cell in the SGZ. (K) The number of proliferating cells as labeled by Rrm1 (arrowheads, G-I) is reduced in DBZ and DAPT treated animals. The average number of Rrm1-positive cells per mm<sup>3</sup> in DAPT-injected animals was used for normalization. (L) The percentage of Rrm1<sup>+</sup> cell colocalizing with Gfap, indicating proliferating glia drops significantly in DBZ- and DAPT-treated experimental groups. Note  $n = 6$  for each experimental group. Asterisks indicate a statistical difference between experimental groups ( $*P < 0.05$ ;  $**P < 0.001$ ; Student's  $t$  test; E, F, K, and L). Error bars represent SEM. (Scale bars: A-C and F-H, 100  $\mu$ m; D and J, 10  $\mu$ m.)

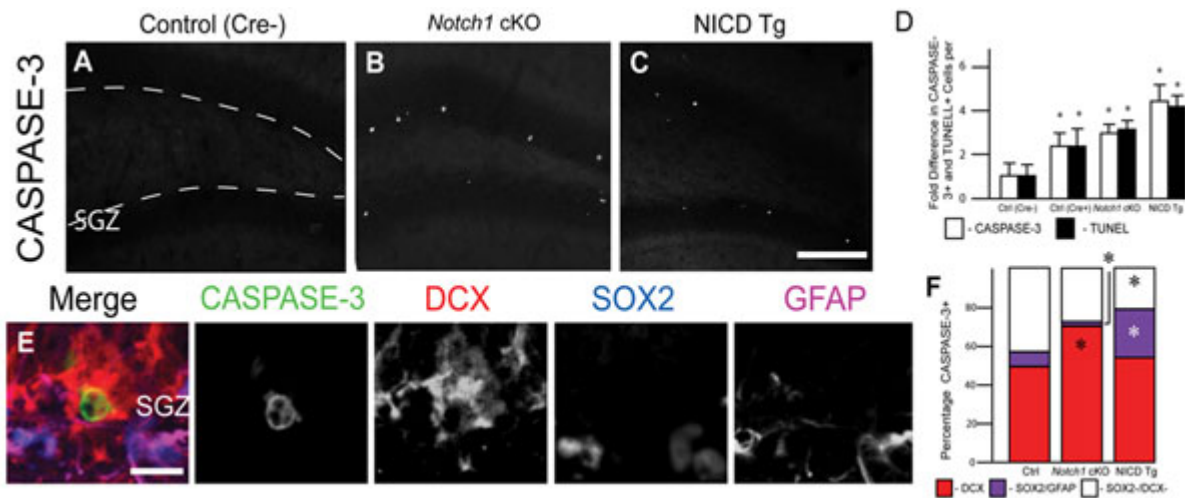


**Fig. 12.** Notch1 levels differentially mediate cell survival. (A-C) Caspase-3 immunostaining for dying cells at P24. (D) Cell death is greatly increased in both NICD Tg and *Notch1* cKO groups when compared with controls. The average number of caspase-3 or TUNEL positive cells per mm<sup>3</sup> in control animals was used for normalization. (E) Confocal image of immunostaining for caspase-3 (green), Dcx (red), Sox2 (blue), and Gfap (magenta). Caspase-3<sup>+</sup> nucleus resides in a Dcx<sup>+</sup> cell body with apparent membrane blebbing. (F) Sox2<sup>+</sup>/Gfap<sup>+</sup> cells die at an increased proportion compared with Sox2<sup>-</sup>/Dcx<sup>-</sup>/Gfap<sup>-</sup> cells in NICD Tg animals versus controls. Similarly, the phenotypic proportions of dying cells in *Notch1* cKO animals is significantly skewed from the control proportions. However, there are several important caveats in interpreting these particular results that are controlled for in other experiments—namely Cre toxicity and NICD transgene toxicity (2-4). Thus, more precise, systematic methods will be needed to determine the exact nature of Notch's influence on cell survival given seemingly conflicting results in the literature (4-7).

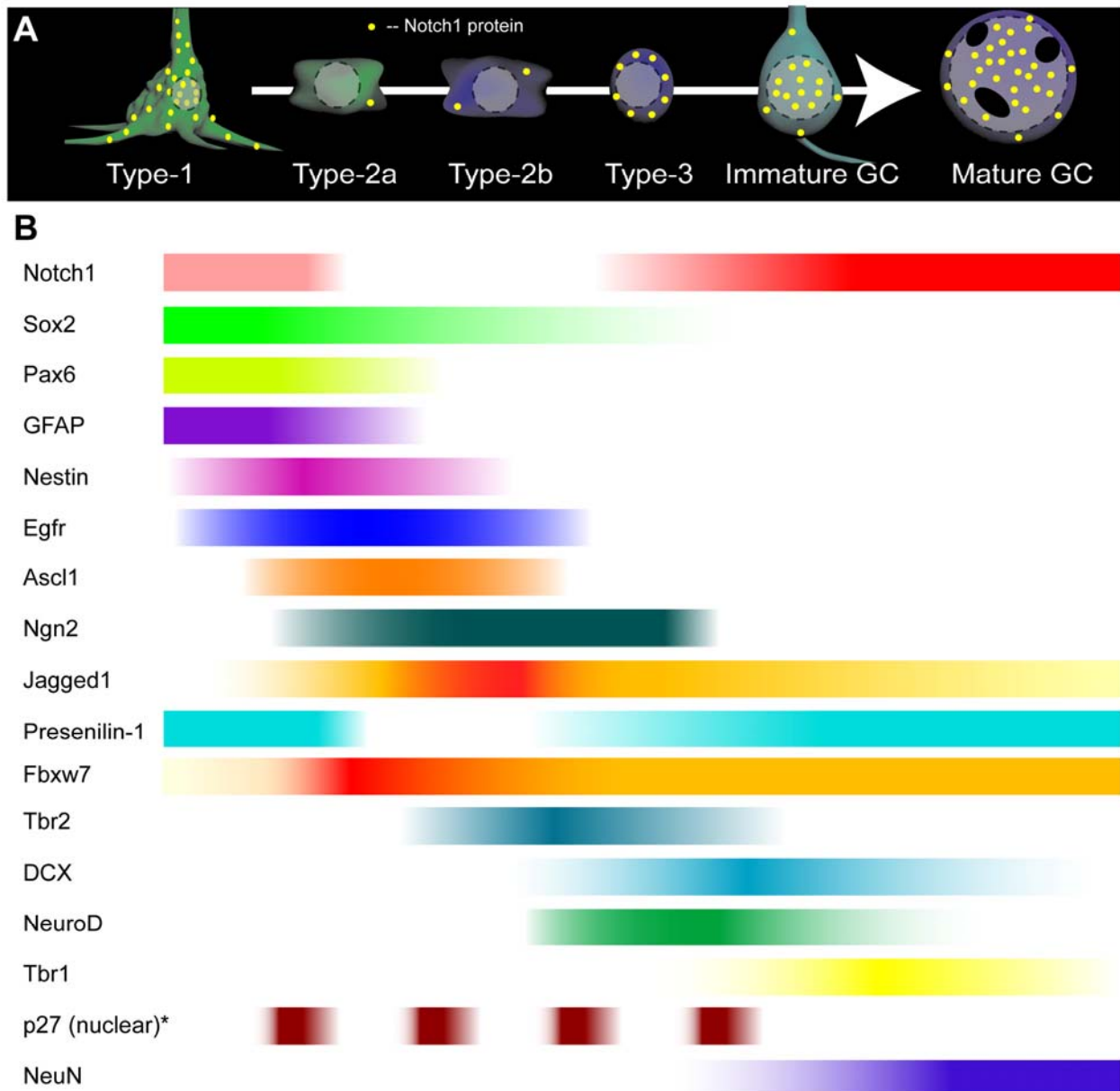


**Fig. 13.** Notch1 subcellular localization and expression gradient of molecules in hippocampal neurogenesis. (A) Subcellular localization of Notch1 protein (yellow) during the generation of a new neuron as it transitions from a radial glial cell to a mature neuron. (B) Schematic of protein expression during this transition based on combinatorial immunostaining of tissue sections. \*Estimation of nuclear p27 protein expression as the subcellular localization appears transient and highly dynamic in these proliferating populations (see SI Fig. 7). Precise experimental quantification of the nuclear p27 levels was therefore not performed.

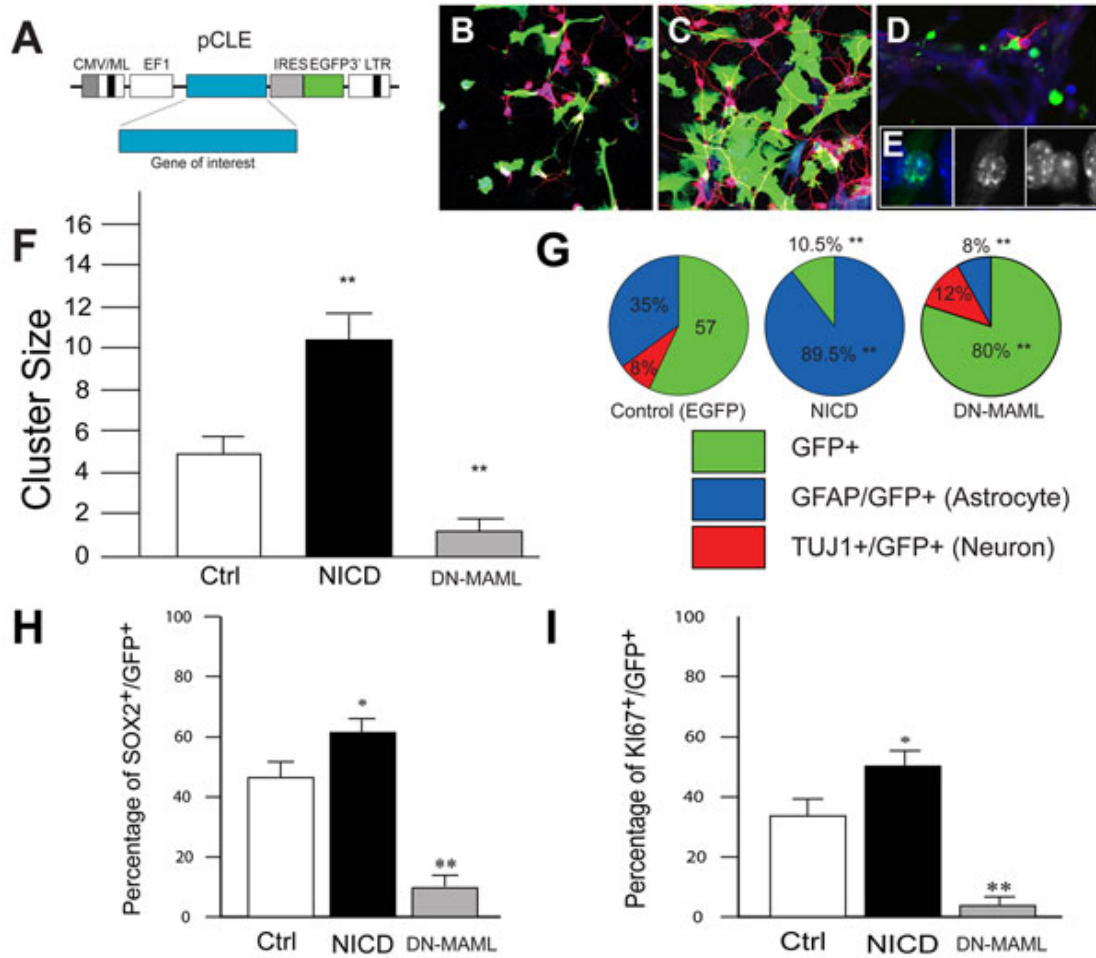


**Fig. 14.** Overexpressing NICD *in vitro* blocks neurogenesis. (A) pCLEG retroviral expression vector. CLEG-NICD virus has human NICD inserted as "Gene of interest." (B, C) Confocal images of neural stem cell culture showing GFP<sup>+</sup>-infected cells (green), TuJ1<sup>+</sup> neurons (red), and DAPI/Gfp (blue). Cells were transduced with CLEG (B) or CLEG-NICD (C) retroviruses or a dominant-negative Mastermind (DN-MAML) construct (D) and cultured for 5 days. (E) DN-MAML-EGFP, like endogenous Mastermind molecules, is localized primarily to the nucleus. (F) Cluster size of infected clones. (G) Phenotypic percentages of infected cells. Percentage of GFP<sup>+</sup> cells expressing Sox2 (H) and Ki67 (I). Asterisks indicate a statistical difference between experimental groups (\* $P < 0.05$ ; \*\* $P < 0.001$ ; Student's *t* test).